sowsky, *Wilhelm Roux' Arch. Entwicklungsmech. Org.* **109**, 70 (1927).
4. W. P. Spencer, *Univ. Tex. Publ.* **5721**, 186 (1947).
5. R. C. Lewontin, *Genetic Basis of the Evolutionary Change* (Columbia Univ. Press, New York, 1974).
6. R. L. Berg, *Genetics* **22**, 225 (1937).
7. A. H. Sturtevant, *Biol. Bull.* **73**, 542 (1937).
8. N. P. Dubinin, *Genetics* **31**, 22 (1946).
9. T. Dobzhansky, B. Spassky, *Genetics* **39**, 472 (1954).
10. S. Kusakabe *et al.*, *Genetics* **154**, 679 (2000).
11. J. R. Powell, *Progress and Prospects in Evolutionary Biology: The* Drosophila *Model* (Oxford Univ. Press, New York, 1997).
12. D. M. Krotoski, D. C. Reinschmidt, R. Tompkins, *J. Exp. Zool.* **233**, 443 (1985).
13. The *L. goodei* experiment was conducted at Florida State University. Materials and Methods are available as supporting material on *Science* Online.
14. Supplementary data for *L. goodei* are available on *Science* Online.
15. The *D. rerio* experiment was conducted at Cornell University. Materials and Methods are available as supporting material on *Science* Online.
16. Supplementary data for *D. rerio* are available on *Science* Online.
17. C. Walker, *Methods Cell Biol.* **60**, 44 (1999).
18. P. Haffter *et al.*, *Development* **123**, 1 (1996).
19. W. Driever *et al.*, *Development* **123**, 37 (1996).
20. M. Rodriguez, W. Driever, *Biochem. Cell Biol.* **75**, 579 (1997).
21. Likelihood analysis was carried out on the vector of counts of lethals observed in each of the J F_1 crosses in the ith sibship, $\mathbf{r}_i = [n_{i1}, n_{i2}, \ldots, n_{ij}]$. R_{io} lethals were observed in the ith cross within each of the I sibships in each species. The log likelihood of a hypothesized mean lethal number R was calculated as

$$\ln L(R) = \sum_{i=1}^{I} \ln \sum_{R_i = R_{io}}^{\infty} P(R_i|R)\,P(\mathbf{r}_i|R_i)$$

where P(.|.) is the conditional probability of the data. Each n_{ij} was assumed to be drawn from a binomial distribution out of an unknown number of lethals R leading to

$$P(\mathbf{r}_i|R_i) = \prod_{j=1}^{J} \frac{R_i!}{\mathbf{r}_{ij}!(R_i - r_{ij})!} 0.25^{r_{ij}} 0.75^{R_{i-r_{ij}}}$$

The distribution of lethal numbers in outbred parents was assumed to be Poisson, with parameter R, so

$$P(R_i|R) = \frac{e^{-2R}(2R)^{R_i}}{R_i!}$$

To find the value of R that maximized ln $L(R)$, we numerically solved $[\delta \ln L(R)]/\delta R = 0$ for R. The values in Tables 1 and 2 were calculated to maximize $P(\mathbf{r}_i|R_i)$.
22. R. R. Humphrey, *Handb. Genet.* **4**, 3 (1975).
23. ———, *J. Hered.* **68**, 407 (1977).
24. D. L. Remington, D. M. O'Malley, *Genetics* **155**, 337 (2000).
25. S. Launey, D. Hedgecock, *Genetics* **159**, 255 (2001).
26. K. Karkkainen, O. Savolainen, V. Koski, *Evol. Ecol.* **13**, 305 (1999).
27. A. J. Wilcox, C. R. Weinberg, D. D. Baird, *N. Engl. J. Med.* **333**, 1517 (1995).
28. N. E. Morton, J. F. Crow, H. J. Muller, *Proc. Natl. Acad. Sci. U.S.A.* **42** 855 (1956).
29. L. E. Licht, L. A. Lowcock, *Comp. Biochem. Physiol. B* **100**, 83 (1991).
30. P. P. Giorgi, M. Fischberg, *Comp. Biochem. Physiol. B* **73**, 839 (1982).
31. J. H. Postlethwait *et al.*, *Genome Res.* **10**, 1890 (2000).
32. M. D. Adams *et al.*, *Science* **287**, 2185 (2000).
33. M. Krawszak *et al.*, *Hum. Mutat.* **15**, 45 (2000).
34. E. S. Lander *et al.*, *Nature* **409**, 860 (2001).
35. A. McLysaght *et al.*, *Yeast* **17**, 22 (2000).
36. J. B. Drost, W. R. Lee, *Environ. Mol. Mutagen.* **25** (suppl. 26), 48 (1995).
37. J. H. Willis, *Heredity* **69**, 562 (1992).
38. O. Ohnishi, *Jpn. J. Genet.* **57**, 623 (1982).
39. J. C. Trexler *et al.*, in *The Everglades, Florida Bay, and Coral Reefs of the Florida Keys: An Ecosystem Sourcebook*, J. W. Porter, K. G. Porter, Eds. (CRC Press, Boca Raton, FL, 2001), pp. 153–181.
40. M. McNeilly helped collect eggs during the *L. goodei* experiment. M. McClure and K. Whitlock generously shared their expertise on maintaining, breeding, and rearing zebrafish. We are grateful to J. Birdsley, S. Ellner, N. Hairston, R. Harrison, and D. Winkler for helpful discussion and/or comments on the manuscript. We thank C. Kearns for advice on a variety of issues; K. Loeffler for help with photography; and R. Carlson, B. Diamond, M. Duffy, O. Duren, T. Sanger, W. Savage, K. Smith, and S. Williams for assistance with zebrafish care. Work on *L. goodei* was funded in part by an NSF dissertation improvement grant to R.C.F. and J.T. (DEB 00-73896) and a grant to J.T. (DEB 99-03925). Funding for the zebrafish work was provided by the NSF (DEB 9981445) to A.R.M.

Supporting Online Material
www.sciencemag.org/cgi/content/full/296/5577/2398/DC1
Materials and Methods
Figs. S1 to S5
Tables S1 to S3

12 March 2002; accepted 16 May 2002

AGTR2 Mutations in X-Linked Mental Retardation

Virginie S. Vervoort,[1] * Michael A. Beachem,[1]* Penny S. Edwards,[1]* Sydney Ladd,[1] Karin E. Miller,[1] Xavier de Mollerat,[1,2] Katie Clarkson,[1] Barbara DuPont,[1,2] Charles E. Schwartz,[1,2] Roger E. Stevenson,[1,2] Ellen Boyd,[3] Anand K. Srivastava[1,2]†

Two angiotensin II (Ang II)–specific receptors, AGTR1 and AGTR2, are expressed in the mammalian brain. Ang II actions on blood pressure regulation, water electrolyte balance, and hormone secretion are primarily mediated by AGTR1. The function of AGTR2 remains unclear. Here, we show that expression of the *AGTR2* gene was absent in a female patient with mental retardation (MR) who had a balanced X;7 chromosomal translocation. Additionally, 8 of 590 unrelated male patients with MR were found to have sequence changes in the *AGTR2* gene, including one frameshift and three missense mutations. These findings indicate a role for AGTR2 in brain development and cognitive function.

Mental retardation (MR) affects 2 to 3% of the human population. Although several causative genes have been identified (*1*), the etiology of MR remains poorly understood. Alterations in molecular pathways involved in neuronal functions, especially cognition, are likely to play an important role.

Angiotensin II (Ang II) and related components of the renin-angiotensin system are largely known for their role in the regulation of blood pressure and water electrolyte balance, and antagonists of the Ang II receptor, as well as angiotensin converting–enzyme inhibitors, are effective therapeutics for hypertension (*2*). This action of Ang II peptide is primarily mediated by one receptor, AGTR1 (*3*). In contrast, the function of a second receptor, AGTR2, which has comparable affinity for Ang II, remains largely unknown. A possible role for AGTR2 in the central nervous system was suggested by the attenuated exploratory behavior and anxiety-like behavior of AGTR2-deficient mice (*4–6*). Results presented here support a role for AGTR2 in human cognitive function.

Linkage of several X-linked MR (XLMR) families to a large genetic interval, Xq23–q25, suggests the presence of one or more MR genes in the region (*1*). One, the *PAK3* gene, has been found to be mutated in MRX30 and MRX47 (*1*). To identify other candidate MR genes, we analyzed a de novo balanced translocation [46, X, t(X;7)(q24;q22)] in a female patient (DF) with moderately severe MR (with an intelligence quotient of 44). The MR phenotype in patient DF is likely due to skewed X inactivation that results in inactivity of both copies of an X-chromosomal gene, one on the inactive normal X chromosome and one on the active translocated X chromosome. We confirmed this idea, determining that X inactivation is totally skewed for one X chromosome (maternal) in patient DF, as compared to random X inactivation in her normal mother (*7*).

We mapped the X-chromosome breakpoint between markers DXS1220 (centromere) and DXS424 (telomere), developing a map of the breakpoint region (fig. S1) (*8*, *9*). Fluorescence in situ hybridization (FISH) with a series of genomic clones from the mapped region (fig. S1) enabled us to map the Xq24 breakpoint to a single P1–artificial chromosome (PAC) clone (dA5O9; approximately 115 kb) (Figs. 1A

[1]J. C. Self Research Institute of Human Genetics, Greenwood Genetic Center, 1 Gregor Mendel Circle, Greenwood, SC 29646, USA. [2]Department of Genetics and Biochemistry, Clemson University, Clemson, SC 29634, USA. [3]Fullerton Genetics Center, Asheville, NC 28803, USA.

*These authors contributed equally to the work.
†To whom correspondence should be addressed. E-mail: anand@ggc.org

and S1) (*9*). No additional genomic rearrangements were detected. The telomeric end of clone dA5O9 was similar to a chromosome X–specific macrosatellite DXZ4 sequence (fig. S1) (*10*). We confirmed the presence of both maternal and paternal alleles of DXZ4 and of five microsatellite markers from the breakpoint critical region (centromere - DXS101 - DXS1220 – breakpoint - DXS8053 - DXS424 - DXS1001 - telomere) in patient DF (*7*, *9*).

Computer-assisted sequence analysis (*8*) of the breakpoint and the adjoining distal regions revealed three potential candidate genes—*PLS3*, *AGTR2*, and *SLC6A14*; two intronless genes, *API5L1* and *HSMT3*; and two likely pseudogenes, *EF1G* and *ASS* (*8*, *11*) (fig. S1). The *PLS3* gene comprises 16 exons spanning about 88 kb. We confirmed the presence of exons 5 to 16 of *PLS3* in the clone dA509 and found by Southern blot analysis that this gene was not disrupted by the X-chromosome breakpoint. This placed the critical breakpoint region between the 3′-end of *PLS3* (fig. S1) and DXZ4, a genomic distance of 77 kb.

Because causative genes are present at long distances from breakpoints in several disease-associated balanced translocations (*12*–*14*), we examined expression of all potential candidate genes, including genes mapping distal to the Xq24 breakpoint, for functional nullisomy in patient DF. Reverse transcription–polymerase chain reaction (RT-PCR) was performed on RNA isolated from lymphoblastoid cell lines or lymphocytes of the patient and a normal male individual (*9*). We obtained specific PCR products corresponding to the *PLS3*, *API5L1*, and *SLC6A14* genes in a normal individual; in patient DF (Fig. 1, B, C, and F); and in her parents (*7*), suggesting that expression of these genes is not affected by the X breakpoint. However, *AGTR2*-specific products were amplified only from control individuals and parents of patient DF, but never from patient DF (e.g., Fig. 1, D and E). These results suggest that both copies of *AGTR2* are silenced in patient DF.

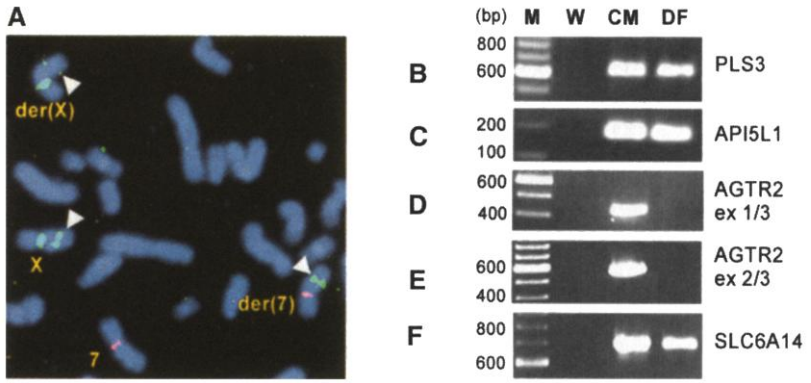

Fig. 1. (**A**) Metaphase spread from the female patient DF with the X;7 translocation showing FISH signals obtained with PAC clone dA5O9 (green signal), with an X-chromosome centromere-specific alphoid sequence probe (green) and chromosome 7–specific probes (red). The hybridization signals (white arrowheads) on both der(X) and der(7) chromosomes indicate that this PAC clone spans the breakpoint. (**B** to **F**) RT-PCR analysis of expression of the *PLS3* (B), *API5L1* (C), *AGTR2* (D) and (E), and *SLC6A14* (F) genes. Primers designed from cDNA sequences were used with RNA isolated from lymphoblasts of a control male (CM) and the female patient (DF) with X;7. W, negative control with no template; M, markers.

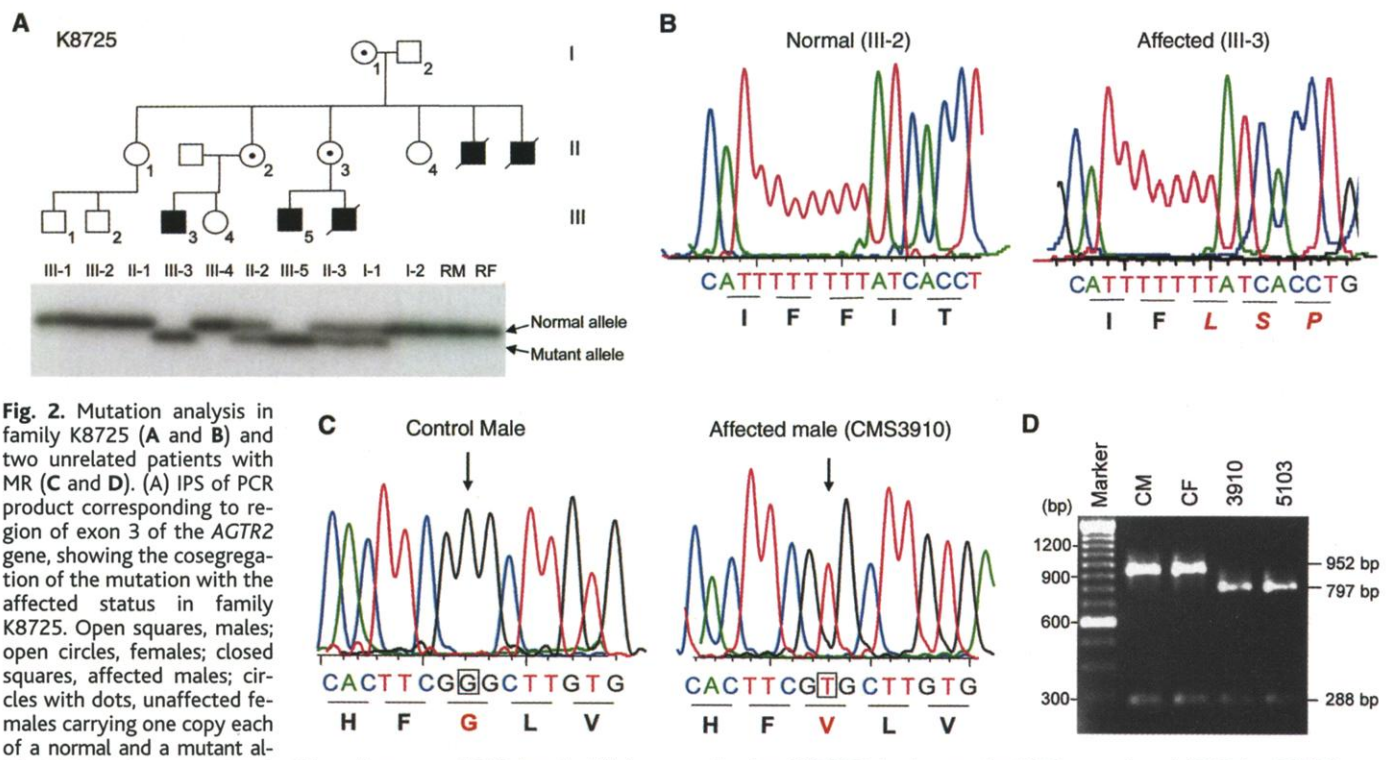

Fig. 2. Mutation analysis in family K8725 (**A** and **B**) and two unrelated patients with MR (**C** and **D**). (A) IPS of PCR product corresponding to region of exon 3 of the *AGTR2* gene, showing the cosegregation of the mutation with the affected status in family K8725. Open squares, males; open circles, females; closed squares, affected males; circles with dots, unaffected females carrying one copy each of a normal and a mutant allele. RM, Random normal male; RF, random normal 395 female. (B) Automated sequence traces showing 402del T, nucleotide sequence, and translated amino acids of normal (III-2) and affected (III-3) males in family K8725 are shown. Amino acids shown in italics (red) are due to a frameshift mutation. (C) Automated sequence traces showing the G62T mutation (indicated by an arrow in the sense strand) in CMS3910 with nonsyndromic MR. (D) Restriction digestion analysis shows that CMS3910 and his affected brother CMS5103, both carry the G62T mutation. A 1240-bp *AGTR2* exon 3 PCR product amplified from genomic DNA was digested with Ase I (common in both control and affected) and Dra III restriction enzymes (generated by the G62T nucleotide alteration) to distinguish between the normal X chromosome (male, CM; and female, CF) and X chromosome of affected brothers (lanes 3910 and 5103). The sizes of the resulting restriction fragments are indicated.

The *AGTR2* gene (*15–17*) is comprised of three exons spanning about 5 kb of genomic DNA. The first two exons encode a 5′-untranslated region, and exon 3 encodes a 363 amino acid transmembrane protein (fig. S1). The *AGTR2* gene maps within clones 1083O19, 517L18, and yWXD338, located distal to the X-chromosome breakpoint (fig. S1).

Southern blot analysis confirmed the structural integrity of the *AGTR2* gene on the translocated chromosome in patient DF. The translocation breakpoint in patient DF lies >150 kb upstream of the *AGTR2* gene (*7*), suggesting that, as in several other human disorders, a critical position effect is caused by a chromosomal rearrangement well outside the transcript region of the disease gene (*12–14*). The effect may result from the separation of distant regulatory elements from the start site of transcription, though sequence analysis of the breakpoint region has not yet revealed any potential regulatory element (*9*). To verify that *AGTR2* was a candidate gene for MR, we looked for mutations in affected males from five families (MRX23, K8045, K8435, K8725, and K8800) putatively assigned to a broad X-chromosomal interval, including the translocation-breakpoint region (*7*, *18*). We also screened (i) affected males from 33 families with possible X-linked MR but no definitive linkage data, and (ii) a large cohort of 552 unrelated male patients with MR of unknown causation but negative for the MR-causing *FMR1* expansion.

We identified one point mutation in *AGTR2* that segregated with MR in family K8725 (*9*, *19*). Two affected males in the family (Fig. 2A) showed deletion of one thymine (T) within a string of eight T's (nt395–nt402). This mutation causes a frameshift at Phe^{133} in the third transmembrane domaine of AGTR2, resulting in a truncated protein (Fig. 2B). We verified heterozygous carrier status in three females in this family (Fig. 2A) (*7*). One unrelated patient (CMS5551), from the group of 552 sporadic males with MR screened, also carried an identical frameshift (del "T") mutation (table S1). This mutation was not present in unaffected family members in family K8725 or in 129 X chromosomes from unaffected Caucasian males.

Three missense changes in *AGTR2* were found in seven sporadic patients with MR (table S1). Patient CMS3910 and his affected elder brother (CMS5103), both with profound MR, carried a G→T transition at nucleotide 62 (Fig. 2, C and D; table S1) that would be predicted to substitute valine for glycine (Gly^{21}→Val), a conserved residue within the AGTR2 extracellular domain (Fig. 3). The same G62T mutation was found in an unrelated male with MR (CMS5044) (table S1).

Three unrelated males with MR carried a G971A (Arg^{324}→Gln) change, and a male with MR carried an A1009G ($Ileu^{337}$→Val) change (table S1; fig. S3), both altering residues in the highly conserved intracellular domain (ICD) of AGTR2. None of these alterations were found in 510 X chromosomes from control males. In addition, we identified four polymorphic variants (742G/A, Arg^{248}→Lys; 498T/C, Leu^{166}→Leu; 695 T/C, Pro^{202}→Pro, and 1011T/A, $Ileu^{337}$→Ileu) of the *AGTR2* gene (table S1).

Five of nine patients with AGTR2 mutations had seizures, and, with the exception of one patient, they were not hypertensive. The MR ranged from moderate to severe, with additional clinical findings in some patients. Such clinical variability, though difficult to explain at this stage, is not an uncommon finding (*1*). Interestingly, two patients, CMS5551 and CMS5044, also showed autistic behavior.

Northern blot analyses of RNA from human brain showed *AGTR2* transcript largely in the cerebellum (fig. S4), complementing an earlier autoradiographic study showing brain localization of Ang II binding (*20*). Indeed a role for AGTR2 in brain development and function had been suspected previously on the basis of its expression in developing and adult brain (*21–23*).

AGTR2 belongs to the seven transmembrane-domain G protein–coupled receptor subfamily (Fig. 3) (*3*). Three of the four MR-causing mutations of AGTR2 are localized in the extracellular and intracellular domain and are present in more than one MR patient (table S1); thus, they may represent critical residues in a functional domain of AGTR2 involved in neuronal signaling. The AGTR2 third intracellular loop is linked to a signaling pathway involving inhibitory G protein (Gi) and extracellular signal-regulated kinase (ERK) inactivation (*3*), and it also interacts with the ErbB3 receptor, which is crucial for the development of Schwann cells (*24*). On a more physiological level, Ang II has been found to elicit AGTR2-mediated increase in voltage-dependent delayed-rectifier K^+ current (I_{KV}) in cultured neurons, an effect mediated by Gi protein activation of phospholipase A2 (*3*, *25*).

In conclusion, our results support the hypothesis that AGTR2 is involved in human brain development. It remains to be seen whether the renin-angiotensin system working through AGTR2 is required for formation or for trophic maintenance of cerebral neuronal connections important for learning and memory.

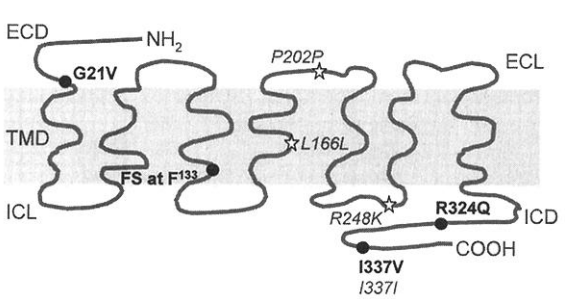

Fig. 3. Putative topology of AGTR2. The sequence changes (indicated by bold type) detected in patients with MR (table S1) is indicated by closed circles, and the polymorphic variants (indicated by italic type) are shown by stars. TMD, transmembrane domain; ECD, extracellular domain; ECL, extracellular loop; ICD, intracellular domain, ICL, intracellular loop; FS, frameshift.

References and Notes

1. J. Chelly, J. L. Mandel, *Nature Rev. Genet.* **2**, 669 (2001).
2. O. Chung, M. Stoll, T. Unger, *Blood Press. Suppl.* **2**, 47 (1996).
3. S. Gallinat, S. Busche, M. K. Raizada, C. Sumners, *Am. J. Physiol. Endocrinol. Metab.* **278**, 357 (2001).
4. L. Hein *et al.*, *Nature* **377**, 744 (1995).
5. T. Ichiki *et al.*, *Nature* **377**, 748 (1995).
6. S. Okuyama *et al.*, *Brain Res.* **821**, 150 (1999).
7. A. R. McCune *et al.*, data not shown.
8. Genomic contigs, clones, markers, and mapping information were obtained from the National Center for Biotechnology Information (www.ncbi.nlm.nih.gov/genome/guide/human) and the Sanger center (www.sanger.ac.uk.HGP) databases. Computer-assisted sequence analysis of contig NT_028405, which includes the entire clone dA509 and spans the translocation breakpoint as well as two distally located contigs NT_025265 and NT_011565, was performed with database search tools and gene prediction software, as implemented in the Nucleotide Identify X package (www.hgmp.mrc.ac.uk/NIX).
9. Supplemental material is available on *Science* Online.
10. J. Giacalone, J. Friedes, U. Francke, *Nature Genet.* **1**, 137 (1992).
11. http://www3.ncbi.nlm.nih.gov/Omim
12. D. J. Kleinjan, V. van Heyningen, *Hum. Mol. Genet.* **7**, 1611 (1998).
13. L. Crisponi *et al.*, *Nature Genet.* **27**, 159 (2001).
14. D. Pfeifer *et al.*, *Am. J. Hum. Genet.* **65**, 111 (1999).
15. D. Lazard *et al.*, *Receptors Channels* **2**, 271 (1994).
16. GenBank accession number NM_000686.
17. Online Mendelian Inheritance in Man entry 300034.
18. R. E. Stevenson, C. E. Schwartz, R. J. Schroer, *X-Linked Mental Retardation* (Oxford Univ. Press, New York, 2000).
19. K. Sossey-Alaoui *et al.*, *Genomics* **60**, 330 (1999).
20. D. P. MacGregor *et al.*, *Brain Res.* **675**, 231 (1995).
21. J. M. Saavedra, *Regul. Pept.* **85**, 31 (1999).
22. A. M. Nuyt *et al.*, *J. Comp. Neurol.* **407**, 103 (1999).
23. J. Ge, N. M. Barnes, *Eur. J. Pharmacol.* **297**, 299 (1996).
24. D. Knowle, S. Ahmed, L. Pulakat, *Regul. Pept.* **87**, 73 (2000).
25. M. Zhu *et al.*, *J. Neurophysiol.* **84**, 2494 (2000).

26. We are grateful to the patients and their family members who participated in this study. We thank S. Daniels, T. Moss, S. Judge, G. F. Guzauskas, K. Hahn, and M. May for technical assistance; T. Wood, F. E. Abidi, R. Nagaraja, C. Skinner, S. Fogle, and R. G. Gregg for sharing expertise, unpublished data, or reagents; and D. Schlessinger and T. Inagami for critically reading the manuscript. Supported by NIH grants RO1-HD39331 and R24 MH57840.

Supporting Online Material

www.sciencemag.org/cgi/content/full/296/5577/2401/DC1
Materials and Methods
Figs. S1 to S4
Table S1

25 March 2002; accepted 11 May 2002